

Statistical Mechanics of DNA-Mediated Colloidal Aggregation

Nicholas A. Licata, Alexei V. Tkachenko

Department of Physics and Michigan Center for Theoretical Physics,
University of Michigan, 450 Church Str., Ann Arbor, Michigan 48109

We present a statistical mechanical model of aggregation in colloidal systems with DNA-mediated interactions. We obtain a general result for the two-particle binding energy in terms of the hybridization free energy G of DNA and two model dependent properties: the average number of available DNA bridges n_i and the effective DNA concentration c_{eff} . We calculate these parameters for a particular DNA bridging scheme. The fraction of all the n -mers, including the infinite aggregate, are shown to be universal functions of a single parameter directly related to the two-particle binding energy. We explicitly take into account the partial ergodicity of the problem resulting from the slow DNA binding-unbinding dynamics, and introduce the concept of angular localization of DNA linkers. In this way, we obtain a direct link between DNA thermodynamics and the global aggregation and melting properties in DNA-colloidal systems. The results of the theory are shown to be in quantitative agreement with two recent experiments with particles of micron and nanometer size. PACS numbers: 81.16.Dn, 82.20.Db, 68.65.-k, 87.14.Gg

I. INTRODUCTION

In the past ten years, there have been a number of advances in experimental assembly of nanoparticles with DNA-mediated interactions([1],[2],[3],[4],[5],[6]). While this approach has a potential of generating highly organized and sophisticated structures([7],[8]), most of the studies report random aggregation of colloidal particles([9],[10]). Despite these shortcomings, the aggregation and melting properties may provide important information for future development of DNA-based self-assembly techniques. These results also have more immediate implications. For instance, the observed sharp melting transition is of particular interest for biosensor applications [11]. For these reasons the development of a statistical mechanical description of these types of systems is of great importance. It should be noted that the previous models of aggregation in colloidal DNA systems were either phenomenological or oversimplified lattice models([12],[13],[14]), which gave only limited insight into the physics of the phenomena.

In this paper, we develop a theory of reversible aggregation and melting in colloidal DNA systems, starting from the known thermodynamic parameters of DNA (i.e. hybridization free energy G), and geometric properties of DNA-particle complexes. The output of our theory is the relative abundance of the various colloidal structures formed (dimers, trimers, etc.) as a function of temperature, as well as the temperature at which a transition to an infinite aggregate occurs. The theory provides a direct link between DNA microscopy and experimentally observed morphological and thermal properties of the system. It should be noted that the hybridization free energy G depends not only on the DNA nucleotide sequence, but also on the salt concentration and the concentration of DNA linker strands tethered on the particle surface[15]. In this paper G values refer to hybridization between DNA free in solution.

In a generic experimental setup, particles are grafted with DNA linker sequences which determine the particle type(A or B). In this paper we will restrict our attention to a binary system¹. These linkers may be flexible or rigid. A selective, attractive potential between particles of type A and B can then be turned on by joining the linkers to form a DNA bridge. This DNA bridge can be constructed directly if the particle linker sequences are chosen to have complementary ends. Alternatively, the DNA bridge can be constructed with the help of an additional linker DNA. This additional linker is designed to have one end sequence complementary to the linker sequence of type A particles, and the other end complementary to type B. The properties of the DNA bridge formed will depend on the hybridization scheme (see figure 1).

The plan for the paper is as follows. In section II.A we provide a description of the problem. In section II.B we determine the bridging probability for the formation of a DNA bridge between two colloids, assuming the known thermodynamic parameters of DNA (hybridization free energy G). Using this bridging probability as input, in section II.C we calculate the effective binding free energy Δ_B for the formation of a dimer. Sections III.A-III.C establish the connection between the theory and the experimentally determined melting profile $f(T)$, the fraction of

¹ This restriction to binary systems is consistent with the current experimental approach. In a recent work we demonstrated that if each particle has a unique linker sequence, one might be able to program mably self-assemble nanoparticle clusters of desired geometry [8].

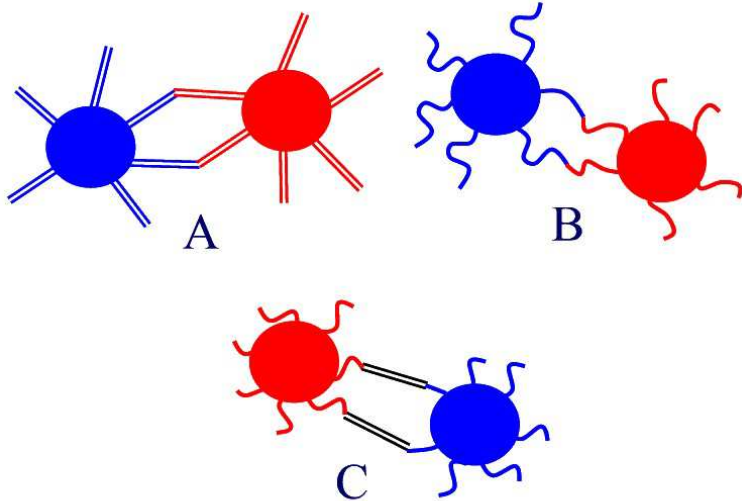


FIG. 1: (Color Online) Graphical depiction of various schemes for DNA bridging. A) A freely-jointed, rigid bridge constructed from complementary linker DNA. B) A flexible bridge can be constructed using complementary linker DNA. C) A rigid bridge constructed from short, flexible linker DNA and a long, rigid linker.

unbound particles as a function of temperature. In particular, we demonstrate how knowledge of A_B can be used to determine this problem, including the effects of particle aggregation. In Section III.D the theory is compared with two recent experiments detailing the reversible aggregation of colloids with DNA-mediated attraction [12], [9]. The main results of the model are summarized in section IV.

II. DNA-MEDIATED INTERACTIONS

A. Description of the problem

We consider particles of type A and B which form reversible AB bonds as a result of DNA hybridization. The task at hand is to determine the relative abundance of the various colloidal structures that form as a function of temperature. From this information we can determine which factors affect the melting and aggregation properties in DNA-colloidal assemblies. To do so we must determine the binding free energy for all of the possible phases (monomer, dimer, ..., infinite aggregate), and then apply the rules for thermodynamic equilibrium. As we will see in section III, these binding free energies can all be simply related to A_B , the binding free energy for the formation of a dimer. Our task is thus reduced to determining A_B from the thermodynamic parameters of DNA and structural properties of the DNA linkers. In our statistical-mechanical framework, A_B is calculated from the model partition function, taking into account the appropriate ensemble averaging for the non-ergodic degrees of freedom. The result is related to the bridging probability for a pair of linkers. By considering the specific properties of the DNA bridge that forms, the bridging probability can be related to the hybridization free energy G of the DNA. In this way, we obtain a direct link between DNA thermodynamics and the global aggregation and melting properties in colloidal-DNA systems.

B. Bridging probability

To begin we relate the hybridization free energy G for the DNA in solution to the bridging probability for a pair of linkers. This bridging probability is defined as the ratio $\frac{P_{\text{bound}}}{P_{\text{free}}}$, with P_{bound} the probability that the pair of linkers have hybridized to form a DNA bridge, and P_{free} the probability that they are unbound. This ratio is directly related to the free energy difference of the bound and unbound states of the linkers \mathcal{G} (throughout this paper we

will use units with $k_B = 1$:

$$\frac{P_{\text{bound}}}{P_{\text{free}}} = \exp \frac{\frac{G}{k_B}}{T} = \frac{c_{\text{eff}}}{c_0} \exp \frac{G}{T} \quad (1)$$

$$c_{\text{eff}} = \frac{\int_{R}^{\infty} \frac{P(r_1; r) P(r_2; r) d^3 r}{R}}{\int_{R}^{\infty} \frac{P(r; r^0) d^3 r}{R^2}} \quad (2)$$

Here $c_0 = 1 \text{M}$ is a reference concentration. $P(r; r^0)$ is the probability distribution function for the linker chain which starts at r^0 and ends at r . The effective concentration c_{eff} is a measure of the change in conformational entropy of the linker DNA as a result of hybridization. It will depend on the properties of the linker DNA (ex: flexible vs. rigid), and the scheme for DNA bridging (ex: hybridization of complementary ends vs. hybridization mediated by an additional linker). c_{eff} is the concentration of free DNA which would have the same hybridization probability as the grafted linkers in our problem. As discussed in section III D, the DNA linker grafting density also plays an important role in determining the possible linker configurations and hence c_{eff} .

Assuming that the size of the linkers is much smaller than the particle radius R , we first consider the problem in a planar geometry. Let the two linkers be attached to two parallel planar surfaces separated by a distance $2h$. Referring to Figure 2 we see that \vec{r} is the location where the linker DNA is grafted onto the particle surface, and \vec{r}' is the position of the free end.

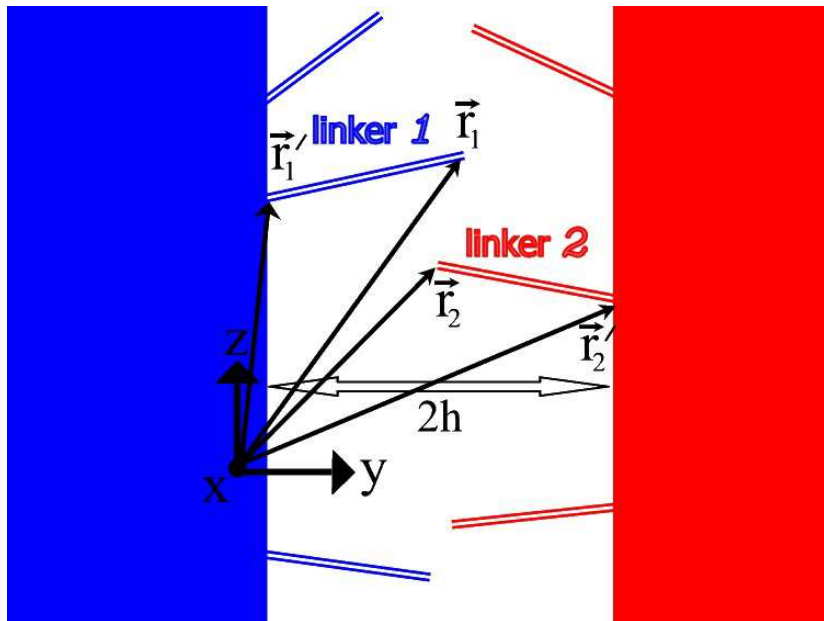


FIG. 2: (Color Online) The statistical weight of a bound state is calculated by determining the number of hybridized configurations for two complementary linker chains relative to the number of unhybridized configurations.

In this paper we consider hybridization by complementary, rigid linker DNA (scheme A in Figure 1). This scheme is particularly interesting since it is directly related to several recent experiments [9], [12]. In a future work we will address other hybridization schemes. We assume that $L < L_p$ and $L \ll R$, where $L_p \approx 50 \text{ nm}$ is the persistence length of ds DNA and L is the ds linker DNA length. In this regime, the linker chains can be treated as rigid rods tethered on a planar surface. The interaction is assumed to be point-like, in which a small fraction $\approx L$ of the linker bases hybridize.

We can calculate the effective concentration by noting that the overlap integral in Eq. (2) is proportional to the volume of intersection of two spherical shells (red and blue circles in Figure 3):

$$c_{\text{eff}} = \frac{2 \pi A}{(2 L^2)^2} = \frac{(L - \frac{r^0}{2} - \frac{r^0}{2})}{2^2 L^2 \frac{r^0}{2} \frac{r^0}{2}}; \quad (3)$$

here $A = \pi r^2 = \pi L^2$ and $r = \sqrt{L^2 - \frac{r^0}{2} - \frac{r^0}{2}} = 4$ (see notations in Figure 3). We have used the fact that $\cos \theta = \frac{r^0}{2} / 2L$. c_{eff} and the binding probability are largest when the linkers are grafted right in front of each other,

i.e. when $r_1^0 = \frac{L}{2} < 2h$. By taking the limit $h \rightarrow L$ we arrive at the following result for the corresponding "bridging" free energy

$$\mathcal{G}_A = G_A + T \log 4 \pi L^3 c_0 : \quad (4)$$

This free energy remains nearly constant for any pair of linkers, as long as they can be connected in principle, i.e. $r_1^0 = \frac{L}{2} < 2L$. This limit is the maximum lateral displacement of the linkers: $r_2 < 2 \frac{L^2}{L^2 - h^2}$, and therefore sets the effective cross-section of the interaction:

$$a = r_2^2 = 4 \pi L^2 h^2 \quad (5)$$

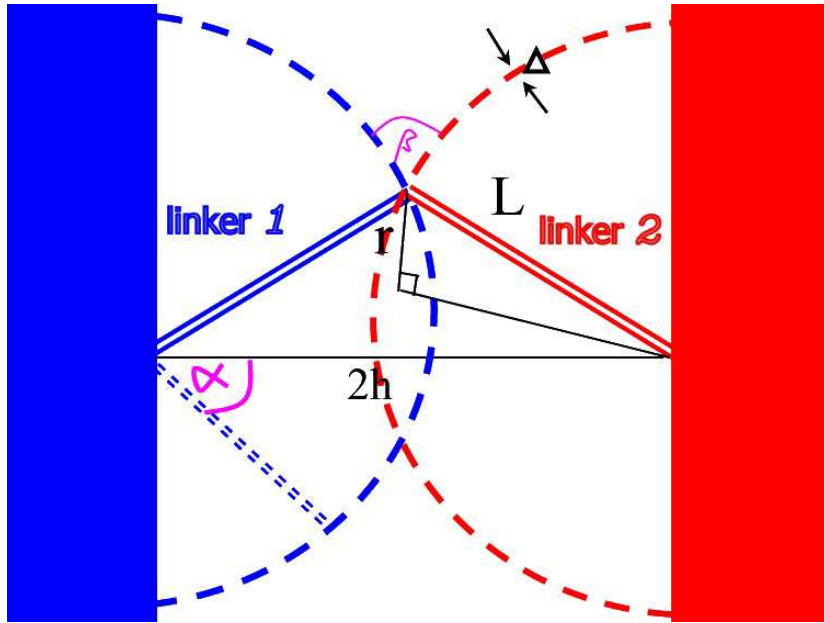


FIG. 3: (Color Online) Cross-sectional view of the hybridization of two complementary rigid linker DNA. The effective concentration is calculated in a planar approximation to the particle surface.

C. Effective binding free energy

We now proceed with the calculation of the effective free energy \mathcal{G}_{AB} , which is associated with the formation of a dimer from a pair of free particles, A and B. Since the DNA coverage on the particle surface is not uniform, this free energy, and the corresponding partition function Z , would in principle depend on the orientations of the particles with respect to the line connecting their centers. The equilibrium binding free energy would correspond to the canonical ensemble of all possible orientations, i.e. $\mathcal{G}_{AB} = -T \log 4 \pi h^2$. However, this equilibrium can only be achieved after a very long time, when the particle pair samples all possible binding configurations, or at least their representative subset. The real situation is different. After the first DNA-mediated bridge is created the particle pair can still explore the configurational space by rotating about this contact point. However, after the formation of two or more DNA bridges (at certain relative orientation of the particles), the further exploration requires multiple breaking and reconnecting of the DNA links, which is a very slow process. We conclude that the system is ergodic with respect to the various conformations of the linker DNA for fixed orientations of the particles, but the orientations themselves are non-ergodic variables. The only exceptions are the single-bridge states: the system quickly relaxes to a more favorable orientational state (unless the DNA coverage is extremely low, and finding a second contact is very hard). If N denotes the number of DNA bridges constituting the AB bond, the appropriate expression for \mathcal{G}_{AB} in this partially ergodic regime is the so-called component averaged free energy ([16], [17]):

$$\mathcal{G}_{AB} = -T \log Z \Big|_{N=2} \quad (6)$$

Each DNA bridge between particles can be either open or closed.

$$Z_{\text{bridge}} = 1 + \exp \frac{\mathcal{G}(h^0; r_i^0, r_j^0)}{T} \quad (7)$$

Here r_i^0 is the 2D position where the bridge is grafted onto surface i . We now consider a generic case when the interaction free energy \mathcal{G} depends on the separation between planar surfaces $2h^0$, and the separation of grafting points r_i^0, r_j^0 , without assumption of a particular bridging scheme. If the probability for bridge formation is small, two DNA linkers on the same surface will not compete for complementary linkers. In this regime the free energy can be calculated by summing over the contribution from each bridge that forms between dimers.

$$F = \frac{1}{T} \sum_{i,j} \log \frac{1 + \exp \frac{\mathcal{G}(h^0; r_i^0, r_j^0)}{T}}{1 + \exp \frac{\mathcal{G}(h^0; r_i^0, r_j^0)}{T}} \quad (8)$$

We convert the summation to integration by introducing the linker areal grafting density a .

$$F = \frac{1}{T} \int_{r_1^0}^Z \int_{r_2^0}^Z \frac{1}{d^2 r_1^0 d^2 r_2^0} \log \frac{1 + \exp \frac{\mathcal{G}(h^0; r_i^0, r_j^0)}{T}}{1 + \exp \frac{\mathcal{G}(h^0; r_i^0, r_j^0)}{T}} \quad (9)$$

Changing variables to $r = r_1^0 - r_2^0$ and $= (r_1^0 + r_2^0)/2$, we can reintroduce the notion of a bridging cross-section $a(h^0)$, this time in a model-independent manner:

$$a(h^0) \log \frac{1 + \exp \frac{\mathcal{G}_0(h^0)}{T}}{1 + \exp \frac{\mathcal{G}(h^0; r)}{T}} = \frac{1}{2} \int_{r_1^0}^Z \int_{r_2^0}^Z \frac{1}{d^2 r \log \frac{1 + \exp \frac{\mathcal{G}(h^0; r)}{T}}{1 + \exp \frac{\mathcal{G}(h^0; r)}{T}}} \quad (10)$$

Here $\mathcal{G}_0(h^0) = \mathcal{G}(h^0; r=0)$ is the minimum free energy with respect to the separation between grafting points r . The factor of $\frac{1}{2}$ arises from the Jacobian for the change of variables. We can now write the free energy:

$$F = \frac{1}{T} \int_{r_1^0}^Z \int_{r_2^0}^Z a(h^0) \log \frac{1 + \exp \frac{\mathcal{G}_0(h^0)}{T}}{1 + \exp \frac{\mathcal{G}(h^0; r)}{T}} \quad (11)$$

We now convert from the planar geometry to the spherical particle geometry using the Debye approximation [18].

$$d^2 = d d \quad (12)$$

$$h^0 = h + \frac{R^2}{2R} \quad (13)$$

Let \mathcal{G}_0 be the minimal value of the bridging free energy. Then the result for F can be rewritten as:

$$F = \frac{1}{T N} \log \frac{1 + \exp \frac{\mathcal{G}_0(h^0)}{T}}{1 + \exp \frac{\mathcal{G}_0(h^0)}{T}} \quad (14)$$

Here N has a physical meaning as the number of potential bridges for given relative positions and orientations of the particles:

$$N = \int_{r_1^0}^Z \int_{r_2^0}^Z a(h^0) \frac{\log \frac{1 + \exp \frac{\mathcal{G}_0(h^0)}{T}}{1 + \exp \frac{\mathcal{G}_0(h^0)}{T}}}{\log \frac{1 + \exp \frac{\mathcal{G}_0(h^0)}{T}}{1 + \exp \frac{\mathcal{G}_0(h^0)}{T}}} \frac{d^2 r_1^0 d^2 r_2^0}{d^2 r} \quad (15)$$

One can calculate the average value of N in terms of the average grafting density, $= h_1 i_1 = h_2 i_2$:

$$h N = \frac{1}{2} \int_{r_1^0}^Z \int_{r_2^0}^Z a(h^0) \frac{\log \frac{1 + \exp \frac{\mathcal{G}_0(h^0)}{T}}{1 + \exp \frac{\mathcal{G}_0(h^0)}{T}}}{\log \frac{1 + \exp \frac{\mathcal{G}_0(h^0)}{T}}{1 + \exp \frac{\mathcal{G}_0(h^0)}{T}}} \frac{d^2 r_1^0 d^2 r_2^0}{d^2 r} \quad (16)$$

In a generic case of randomly grafted linkers, hN i completely defines the overall distribution function of N , which must have a Poisson form: $P(N) = \frac{hN^i e^{-hN}}{N!}$. The average number of bridges hN i between two particles depends on both the DNA linker grafting density and the bridging probability determined from \mathcal{G} .

The free energy for the formation of a dimer $A_B = hF i_{2+} - T \log$. The second term is the entropic contribution to the free energy, which comes from integration over the orientational and translational degrees of freedom of the second particle. Because the system is not ergodic in these degrees of freedom, the accessible phase space will be reduced by a factor of P_{2+} . P_{2+} is the probability that there are at least two DNA bridges between the particles. In terms of the average number of bridges hN i between particles, we have the following relations:

$$P_{2+} = 1 - (1 + hN i) e^{-hN i} \quad (17)$$

$$hN i_{2+} = \frac{hN i - 1 - e^{-hN i}}{P_{2+}} \quad (18)$$

$$A_B = T \left(hN i_{2+} \log \frac{1 + \exp \left(\frac{-\mathcal{G}}{T} \right)}{1 + \exp \left(\frac{-\mathcal{G}}{T} \right)} + \log P_{2+} \right) + \log \frac{4}{(2R)^2 c_0} \quad (19)$$

Here h is the localization length of the A_B bond, which comes from integrating the partition function over the radial distance between particles.

We now can calculate hN i for the case of freely-jointed rigid bridging considered earlier (i.e. for scheme A). In a previous section we provided a direct calculation of the interaction free energy, $\mathcal{G}_0(h) = \text{const} - \mathcal{G}$ (eq.4), and bridging cross-section, $a(h^0) = 4(L^2 - h^2)$. Applying eq. 16 we arrive immediately at the following result.

$$hN i = 8 \int_0^{L^2} 2^2 R (L^2 - h^2) dh^0 = \frac{16^2 2^2 R L^3}{3} \quad (20)$$

Having determined the free energy, we are now in a position to determine the melting properties for DNA colloidal assemblies.

III. AGGREGATION AND MELTING IN COLLOIDAL-DNA SYSTEMS

At this stage of the paper we have calculated the binding free energy A_B for an A_B pair, starting with the thermodynamic parameters of DNA (hybridization free energy \mathcal{G}). In this section of the paper we establish the connection between that result and the experimentally observable morphological behavior of a large system. One of the ways to characterize the system is to study its melting profile ($\phi(T)$), which is the fraction of unbound particles as a function of temperature. To determine the profile we calculate the chemical potential for each phase (monomer, dimer, etc.) and apply the thermodynamic rules for phase equilibrium. We will demonstrate how the single binding free energy A_B can be used to determine the contribution of each phase to the melting profile, including the effects of aggregation.

A. Dimer formation

To begin we discuss the formation of dimers via the reaction $A + B \rightleftharpoons A_B$. We can express the chemical potential of the i^{th} species i in terms of the particle concentrations $c_i = \frac{N_i}{V}$.

$$\mu_A = T \log(c_A) \quad (21)$$

$$\mu_B = T \log(c_B) \quad (22)$$

$$\mu_{A_B} = T \log(c_{A_B}) + \mu_A - \mu_B \quad (23)$$

Here μ_{A_B} is the binding free energy for the formation of a dimer. In terms of the potential $V(r)$ between A and B type particles we have:

$$\mu_{A_B} = T \log \int_0^{\infty} 4 (2R)^2 c_0 dr \exp \left(-\frac{V(r)}{T} \right) \quad (24)$$

In this section we are not particularly concerned with the specific form of the DNA-induced potential $V(r)$, having already determined χ_{AB} in the previous section. We simply note that the prefactor $4/(2R)^2$ arises since the interaction is assumed to be isotropic, with R the particle radius. Equilibrating the chemical potential of the various particle species, we obtain the condition for chemical equilibrium.

$$A + B = AB \quad (25)$$

The result is a relationship between the concentration of dimers and monomers.

$$c_{AB} = \frac{c_A c_B}{c_0} \exp \frac{\chi_{AB}}{T} \quad (26)$$

The overall concentration of particles in monomers and dimers must not differ from the initial concentration.

$$c_A^i = c_A + c_{AB} \quad (27)$$

$$c_B^i = c_B + c_{AB} \quad (28)$$

If the system is prepared at equal concentration, $c_A^i = c_B^i = \frac{1}{2}c_{\text{tot}}$, subtracting the two equations we see that $c_A = c_B = c$. Written in terms of the fraction of unbound particles $f = \frac{c}{2c_{\text{tot}}}$ we have a quadratic equation for the unbound fraction.

$$1 = f + \exp \frac{\chi_{AB}}{T} f^2 \quad (29)$$

To simplify we have defined an effective free energy e_{AB} for the formation of a dimer.

$$e_{AB} = \chi_{AB} - T \log \frac{c_{\text{tot}}}{2c_0} \quad (30)$$

The solution for the fraction of unbound particles as a function of temperature is simply:

$$f = \frac{1 + \frac{1 + 4 \exp \frac{e_{AB}}{T}}{2 \exp \frac{e_{AB}}{T}}}{1 + \frac{1 + 4 \exp \frac{e_{AB}}{T}}{2 \exp \frac{e_{AB}}{T}}} \quad (31)$$

Previous studies [9] only included the dimer contribution to the melting properties of DNA colloidal assemblies. With the basic formalism at hand, we can now extend the preceding analysis to include the contribution of trimers and tetramers.

B. Trimers and tetramers

Now consider the formation of a trimer via $2A + B \rightleftharpoons ABA$. The chemical potential is slightly different in this case.

$$\chi_{ABA} = T \log (c_{ABA}) + \chi_{ABA} \quad (32)$$

Taking into account that there are now two AB bonds in the structure, one might conclude that $\chi_{ABA} = 2\chi_{AB}$. This is not quite correct, since there is a reduction in solid angle available to the third particle. To form a trimer, an AB bond forms first, which contributes χ_{AB} to χ_{ABA} . Some simple geometry shows that the remaining A particle only has 3 steradians of possible bonding sites to particle B. Making this change in the prefactor of eq. 24, one can see that the second bond contributes $\chi_{AB} - T \log \frac{3}{4}$ to χ_{ABA} .

$$\chi_{ABA} = 2\chi_{AB} - T \log \frac{3}{4} \quad (33)$$

The equation for chemical equilibrium can once again be expressed in terms of the particle concentrations.

$$2A + B = ABA \quad (34)$$

$$c_{ABA} = \frac{3}{4} \frac{c_A^2 c_B}{c_0^2} \exp \frac{-2\chi_{AB}}{T} \quad (35)$$

To include the trim er contribution, we note that there are two possible varieties, with $c_{ABA} = c_{BAB}$.

$$c_A^i = c_A + c_{AB} + 2c_{ABA} + c_{BAB} \quad (36)$$

$$c_B^i = c_B + c_{AB} + c_{ABA} + 2c_{BAB} \quad (37)$$

Following the same line of reasoning as before, the resulting equation for the unbound fraction f is:

$$1 = f + \exp \frac{q_B}{T} f^2 + \frac{9}{4} \exp \frac{2q_B}{T} f^3 \quad (38)$$

For tetramers we will follow the same general reasoning, however in this case there are two different structure types. The reaction $2A + 2B \rightarrow ABA + BAB$ results in the formation of string like structures.

$$c_{ABA} = T \log (c_{ABA}) + c_{ABA} \quad (39)$$

As in the trim er case, the last particle has 3 steradians of possible bonding sites, and contributes $c_{ABA} = T \log \frac{3}{4}^2$ to c_{ABA} .

$$c_{ABA} = 3 c_{AB} T \log \frac{3}{4}^2 \quad (40)$$

$$2A + 2B = c_{ABA} \quad (41)$$

$$c_{ABA} = \frac{3}{4}^2 \frac{c_A^2 c_B^2}{c_o^3} \exp \frac{3 c_{AB}}{T} \quad (42)$$

If an A type particle approaches a trim er of variety ABA , a branched structure can result. The reaction $3A + B \rightarrow AAAB$ results in the formation of these branched structures.

$$c_{AAAB} = T \log (c_{AAAB}) + c_{AAAB} \quad (43)$$

For the branched case, the last particle has approximately 2 steradians of possible bonding sites, and contributes $c_{AAAB} = T \log \frac{1}{2}$ to c_{AAAB} .

$$c_{AAAB} = 3 c_{AB} T \log \frac{3}{8} \quad (44)$$

$$3A + B = c_{AAAB} \quad (45)$$

$$c_{AAAB} = \frac{3}{8} \frac{c_A^3 c_B}{c_o^3} \exp \frac{3 c_{AB}}{T} \quad (46)$$

To include all of the tetramer contributions, note that there are two branched varieties, with $c_{AAAB} = c_{BBBA}$. Finally we impose the constraint that the initial particle concentrations do not differ from the concentration of all the trimers, for $n=1,2,3,4$.

$$c_A^i = c_A + c_{AB} + 2c_{ABA} + c_{BAB} + 2c_{ABA} + 3c_{AAAB} + c_{BBBA} \quad (47)$$

$$c_B^i = c_B + c_{AB} + c_{ABA} + 2c_{BAB} + 2c_{ABA} + 3c_{AAAB} + 3c_{BBBA} \quad (48)$$

The final result is an equation for the unbound fraction f expressed entirely in terms of the effective free energy q_B of a dimer.

$$1 = f + \exp \frac{q_B}{T} f^2 + \frac{9}{4} \exp \frac{2q_B}{T} f^3 + \frac{21}{8} \exp \frac{3q_B}{T} f^4 \quad (49)$$

For high temperatures, the melting problem is governed by the solution to this polynomial equation for f . For temperatures below the melting point we expect to find particles in large extended clusters. We now proceed to calculate the equilibrium condition between monomers in solution and the aggregate.

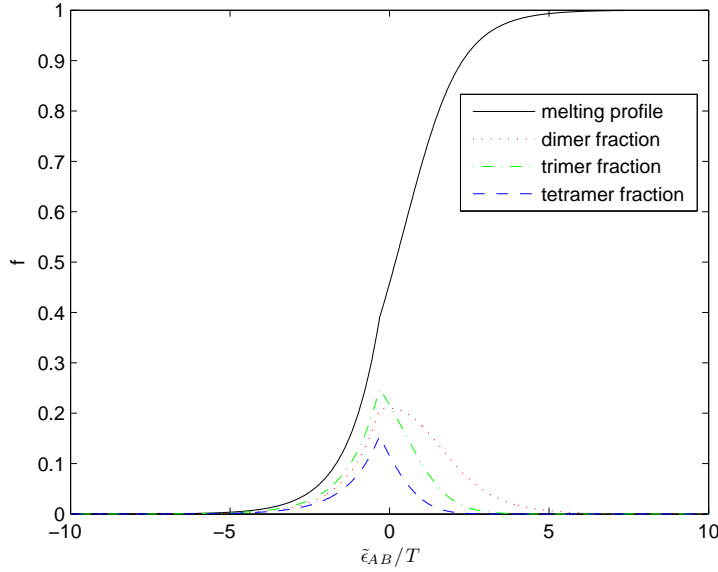


FIG. 4: (Color Online) The actual unbound fraction f is the concatenation of the aggregate profile for $T < T_c$ and the n-mer profile for $T > T_c$. The fraction of particles in dimers, trimers, and tetramers is also plotted.

C. Reversible sol-gel transition

To understand the basic structure of the aggregate, we simply note that there are many DNA attached to each particle. This gives rise to branching, as in the discussion of possible tetramer structures. Since the DNA which mediate the interaction are grafted onto the particle surface, once two particles are bound, the relative orientation of the pair is essentially fixed. The resulting aggregate is a tree-like structure, and the transition to an infinite aggregate at low temperatures is analogous to the sol-gel transition in branched polymers[19].

Particles in the aggregate are pinned down by their nearest neighbor bonds, so we do not consider their translational entropy. As a result the chemical potential is simply $\mu_1 = \mu_1$. Equilibrating the chemical potential of the monomer in solution and in the aggregate we have:

$$T \log (c) = \mu_1 \quad (50)$$

$$\mu_1 = \mu_{AB} - T \log (\mu_1) \quad (51)$$

Here μ_1 , μ_1 is the configurational entropy of the branched aggregate, per particle.

The concentration of particles in the aggregate c_1 is the total concentration c minus the n-mer concentration. Here $c_1 = c_A + c_B$ is the total monomer concentration, $c_2 = c_{AB}$ is the total dimer concentration, etc.

$$c_1 = c_{tot} - c_A - c_B - c_{AB} \quad (52)$$

Expressed in terms of ϵ_{AB} and the fraction of solid angle available to particles in the aggregate $\mu_1 = \frac{1}{4}$ we have:

$$f_1 = \frac{1}{4} \exp \frac{\epsilon_{AB}}{T} \quad (53)$$

The transition from dimers, trimers, etc. to the aggregation behavior is the temperature T_c at which $f_1(T_c)$ is a solution to eq. 49. In words, T_c is the temperature at which the aggregate has a non-zero volume fraction. The fraction of unbound particles for these colloidal assemblies will be governed by eq. 53 for $T < T_c$ and eq. 49 for $T > T_c$. As claimed, we can simply relate the unbound fraction to ϵ_{AB} for both n-mers and the aggregate.

D. Comparison to the experiment

Let's consider the experimental scheme of Chaikin et al[9]. In the experiment, $R = 5$ μm polystyrene beads were grafted with dsDNA linkers of length $L = 20$ nm. The 11 end bases of the A and B type particles were single stranded

and complementary. We have already determined the bridging probability in this scenario (see section II.B). In the experiment [9] a polymer brush is also grafted onto the particle surface, which will have the effect of preferentially orienting the rods normal to the surface (See Figure 3). This constraint of the linker DNA can be incorporated quite easily into our results for G and hNi . Returning to section II.B, when integrating over linker conformations we simply constrain each rigid rod to a cone of opening angle 2θ . The upper bound for the polar integration is now as opposed to .

$$G_A' = G_A + T \log 4 \pi L^3 c_0 (1 - \cos \theta)^2 \quad (54)$$

The alignment effect should also be taken into account when calculating hNi . If the particles are separated by less than $2L \cos \theta$ the end sequences will be unable to hybridize. Following the same steps as before, the lower bound for the hNi integration is now $L \cos \theta$ as opposed to 0.

$$hNi = 8 \pi^2 R^2 (L^2 - h^2) dh^0 \quad (55)$$

$$= \frac{16}{3} \pi^2 R^2 L^3 \frac{h^2}{1 + \frac{\cos \theta}{2} (\cos^2 \theta - 3)} \quad (56)$$

In the absence of the brush, and at sufficiently low linker grafting density ρ , the alignment effect could be removed by setting $\theta = \frac{\pi}{2}$, in which case we recover our previous results. Since the polymer brush is stiff, it also imposes a minimum separation of $2h$ between particles, where h is the height of the brush. As a result, in the expression for G_{AB} we can approximate the radial flexibility of the AB bond as $\rho' L \approx h$.

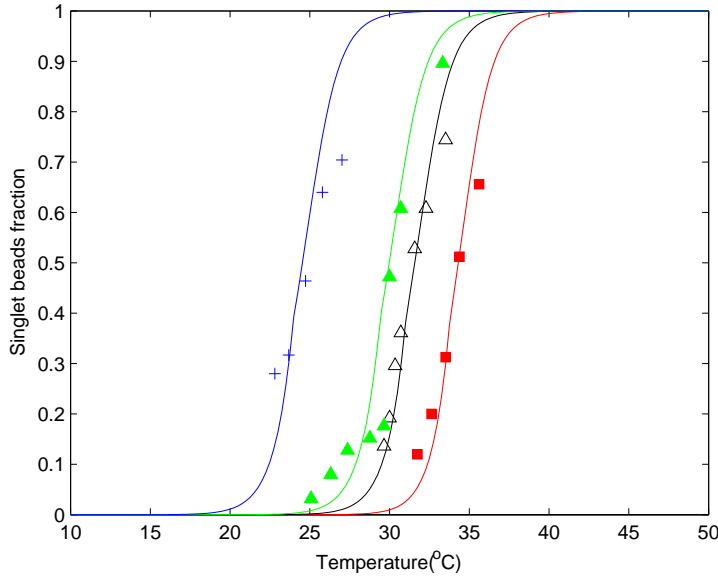


FIG. 5: (Color Online) Comparison of the melting curves $f(T)$ determined by our model to the experimental data of Chaikin et al (See Fig 2 in [9]). The four data sets are for the four different polymer brushes used. For the model fits we find that $hNi_{2+} = 2.01$ for crosses, 2.07 for solid triangles, 2.13 for empty triangles, and 2.35 for squares.

We have now related the free energy G_{AB} to the known thermodynamic parameters of DNA ($G = H - T S$, $H = 77.2 \frac{\text{kcal}}{\text{mol}}$ and $S = 227.8 \frac{\text{cal}}{\text{molK}}$), and the properties of linker DNA chains attached to the particles (grafting density $\rho' = 3 \times 10^8 \frac{\text{DNA}}{\text{m}^2}$ and linker length $L' = 20\text{nm}$). The height of the polymer brush is $h = 13 - 5\text{nm}$ [9].

In fitting the experimental data we have taken the average value $hNi = 13\text{nm}$. Changing h within these bounds does not have a major effect on the melting curves. As a result there is one free parameter in the model, the constraint angle θ . This angle determines hNi and G , which in turn determine e_{AB} , and finally the melting profile.

With some minor modifications we can also analyze the "tail to tail" hybridization mode in a recent experiment of Mirkin et al [12]. In this experiment, $R = 6.5\text{nm}$ gold nanoparticles were chemically functionalized with ssDNA linkers. The last 15 bases on the markers for particles of type A and B were chosen to be complementary to a 30 base ssDNA linker. Since the strands are not ligated after hybridization, the experimental pictures are similar.

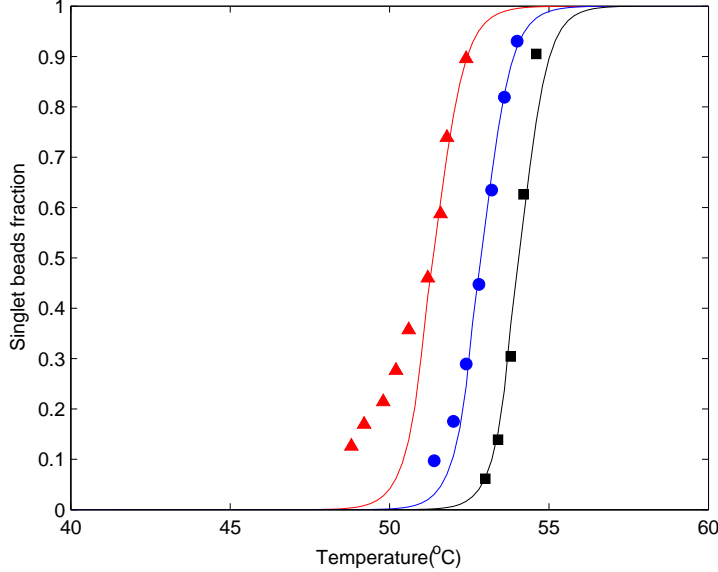


FIG. 6: (Color Online) The effect of the linker DNA grafting density on the melting profile (T). The results of the model are compared with experimental data in [12]. The three data sets represent grafting densities of 100% (squares), 50% (circles), and 33% (triangles) for which $hNi_{2+} = 2.32, 2.16$, and 2.05 respectively.

The unhybridized portion of the ssDNA linker simply serves as a spacer, and the hybridized portions become dsDNA, which we can again treat as rigid rods (see section II B). This experiment is done without the addition of a polymer brush, but the grafting density is two orders of magnitude larger than the experiment of Chaikin et al. As a result, there is still an entropic repulsion [7] associated with compressing the particles below separation $2h$. Here h could loosely be interpreted as the radius of gyration of the unhybridized portion of the linker. Despite the fact that $L = R$, our planar calculation of G provides a good fit to the experimental data. The other major difference is that now the attraction between particles is mediated by an additional DNA linker.

$$G = G_A + G_B - T \log \frac{c_{\text{link}}}{c_0} \quad (57)$$

The first term is the contribution to the free energy from the hybridization of the end sequence on linker A to the complementary portion of the 30 base ss linker. The hybridization free energies G_A and G_B were calculated with the DINAMelt web server [20]. The last term is the contribution to the free energy from the translational entropy of the additional linker DNA, with c_{link} the additional linker concentration. This highlights some incorrect assumptions of the thermodynamic melting model [12], where the two hybridization free energies were not calculated separately, and the translational entropy of the additional linker DNA was ignored. By introducing diluent strands to the system, one can probe the effect of the linker grafting density on the melting properties of the assembly (See Figure 2B in [12]). The agreement between the experimental data and our theory is good, except at small f values. This is not surprising, since comparing the two requires relating the measurement of optical extinction to the unbound fraction f . This is a nontrivial matter when dealing with aggregation, which corresponds to the small f regime.

IV. CONCLUSION

We have developed a statistical mechanical description of aggregation and melting in DNA-mediated colloidal systems. First we obtained a general result for two-particle binding energy in terms of DNA hybridization free energy G , and two model-dependent parameters: the average number of available bridges hNi and the effective DNA concentration c_{eff} . We have also shown how these parameters can be calculated for a particular bridging scheme. In our discussion we have explicitly taken into account the partial ergodicity of the problem related to slow binding-unbinding dynamics.

In the second part of the paper it was demonstrated that the fractions of dimers, trimers and other clusters, including the infinite aggregate, are universal functions of a parameter $g_B = T = \frac{1}{AB} = T \log \left[\frac{c_{\text{tot}}}{2c_0} \right]$. We have applied the results of our theory to a particular scheme when the DNA bridge is made of two freely jointed rods (dsDNA). The obtained melting curves are in excellent agreement with two types of experiments, done with particles of nanometer and micron sizes. Furthermore, our analysis of the experimental data give an additional insight into microscopic physics of DNA bridging in these systems: it was shown that the experiments cannot be explained without introduction of angular localization of linkers dsDNA. The corresponding localization angle θ is the only fitting parameter of the model, which allows one to fit both the position and width of the observed melting curves.

There are several manifestations of the greater predictive power of our statistical mechanics approach, compared to the earlier more phenomenological models. First, once θ is determined for a particular system, our theory allows one to calculate the melting behavior for an alternative choice of DNA linker sequences. Second, if the resulting clusters are separated, for example in a density gradient tube, the relative abundance of dimers, trimers, and tetramers can be compared to the values determined from the theory.

Finally, the theory predicts aging of the colloidal structures, one experimental signature for which is hysteresis of the melting curves. Such an experiment proceeds by preparing a system above the melting temperature, and measuring the unbound fraction of colloids as the temperature is lowered. The system is allowed to remain in this cooled state for a very long time, perhaps months, during which multiple DNA bridges break and reform. During this time the colloids relax into a more favorable orientation state, including states which are not accessible by simply rotating about the contact point formed by the first DNA bridge between particles. This favorable orientation state is characterized by an average number of DNA bridges hN greater than what we calculate in the partially ergodic regime. If the unbound fraction is then measured as the temperature is increased, the melting curve will shift to a higher temperature, consistent with a larger value of hN .

V. ACKNOWLEDGMENTS

This work was supported by the ACS Petroleum Research Fund (grant PRF # 44181-AC10), and by the Michigan Center for Theoretical Physics (award # MCTP 06-03).

[1] Mirkin, C. A.; Letsinger, R. L.; Masic, R. C.; Storho, J. J. *Nature* 1996, 382, 607–609.
 [2] Storho, J. J.; Mirkin, C. A. *Chem. Rev.* 1999, 99, 1849.
 [3] Masic, R. C.; Storho, J. J.; Mirkin, C. A.; Letsinger, R. L. *J. Am. Chem. Soc.* 1998, 120, 12674.
 [4] Masic, R. C.; Mirkin, C. A.; Letsinger, R. L. *J. Am. Chem. Soc.* 2000, 122, 6305.
 [5] Alivisatos, A. P.; Peng, X.; Wilson, T. E.; Johnsson, K. P.; Loweth, C. J.; Jr., M. P. B.; Schultz, P. G. *Nature* 1996, 382, 609.
 [6] Braun, E.; Eichen, Y.; Sivan, U.; Ben-Yoseph, G. *Nature* 1998, 391, 775.
 [7] Tkachenko, A. V. *Physical Review Letters* 2002, 89, 148303.
 [8] Licata, N. A.; Tkachenko, A. V. *arXiv:cond-mat/0504407 v2* 2006, .
 [9] Valignat, M. P.; Theodoly, O.; Crocker, J. C.; Russel, W. B.; Chaikin, P. M. *PNAS* 2005, 102, 4225–4229.
 [10] Biancaniello, P. L.; Kim, A. J.; Crocker, J. C. *PRL* 2005, 94, 058302.
 [11] Park, S.-J.; Taton, T. A.; Mirkin, C. A. *Science* 2002, 295, 1503.
 [12] Jin, R.; Wu, G.; Li, Z.; Mirkin, C. A.; Schatz, G. C. *JACS* 2003, 125, 1643–1654.
 [13] Lukatsky, D.; Frenkel, D. *Physical Review Letters* 2004, 92, 068302.
 [14] Park, S. Y.; Stroud, D. *Phys. Rev. B* 2003, 67, 212202.
 [15] Vainrub, A.; Pettitt, B. M. *Physical Review E* 2002, 66, 041905.
 [16] Thirumalai, D.; Mountain, R. D.; Kirkpatrick, T. R. *Physical Review A* 1989, 39, 3563–3574.
 [17] Palmer, R. G. *Advances in Physics* 1982, 31, 669–735.
 [18] Israelachvili, J. N. *Intermolecular and Surface Forces: With Applications to Colloidal and Biological Systems*; Academic Press Inc.: London, 1985.
 [19] de Gennes, P. *Scaling Concepts of Polymer Physics*; Cornell University Press, Ithaca, NY : Ithaca, NY, 1979.
 [20] Markham, N. R.; Zuker, M. *Nucleic Acids Res.* 2005, 33, W 577–W 581.